Influence of depth, focal mechanism, and tectonic setting on the shape and duration of earthquake source time functions

Article *in* Journal of Geophysical Research Atmospheres · June 2001

DOI: 10.1029/2000JB900468

CITATIONS
99

READS
236

1 author:

Heidi Houston
University of Washington Seattle
81 PUBLICATIONS **3,253** CITATIONS

SEE PROFILE

JOURNAL OF GEOPHYSICAL RESEARCH, VOL. 106, NO. B6, PAGES 11,137–11,150, JUNE 10, 2001

Influence of depth, focal mechanism, and tectonic setting on the shape and duration of earthquake source time functions

Heidi Houston

Department of Earth and Space Sciences, University of California, Los Angeles, California

Abstract. Source time functions of 255 moderate to great earthquakes obtained from inversions of teleseismic body waves by *Tanioka and Ruff* [1997] and coworkers were compared in a systematic way. They were scaled to remove the effect of moment and to allow the direct comparison and averaging of time function shape as well as duration. Time function durations picked by *Tanioka and Ruff* [1997] are proportional to the cube root of seismic moment if moments from the Harvard centroid moment tensor catalog are used. The average duration of scaled time functions is shorter and the average shape has a more abrupt termination for deeper events than shallower ones, with a distinct change occurring at ~40 km depth. The complexity of the time functions, as quantified by the number of subevents, appears to decrease below ~40 km depth. Furthermore, among events shallower than 40 km, the average duration of scaled time functions is shorter, and their average shape has a more abrupt termination (1) for events with strike-slip focal mechanisms compared to thrust events and (2) for the few thrust events associated with an intraplate setting compared to the majority associated with an interplate (subduction) boundary. In each of these cases, events in more tectonically and seismically active settings have a longer duration and a more gradual termination. This can be interpreted in terms of lower stress drops and/or slower rupture velocities at active plate boundaries, suggesting that fault rheology depends on slip rate and may evolve as total fault slip accumulates. Furthermore, differences in average time function shape and duration associated with different subduction zones suggest that differences exist in the rheology on the plate boundaries at the various subduction zones.

1. Introduction

The manner in which earthquake ruptures initiate, propagate and terminate is central to the process of seismic faulting. A primary avenue of investigation is through earthquake source time functions, which have been extensively studied for several decades (see *Kanamori* [1986] for a review). An earthquake source time function is a time series that specifies the rate of the seismic moment release during an earthquake. The time function is proportional to slip, spatially integrated over the fault plane, as a function of time; ideally, one would like to know the complete spatiotemporal history of slip at every point on the fault plane, but this is much harder to resolve from seismograms.

Recently, a catalog containing source time functions of more than 250 earthquakes has been available over the Internet. Some basic properties of the catalog (as of June 1996 when it contained 99 events), including the moment dependence of duration and peak moment release rate, were reported by *Tanioka and Ruff* [1997]. Here I analyze the now larger catalog (255 events available as of December 2000) to reexamine some of their conclusions and to extract more information about source scaling and the shape of time functions. Part of the study employs a scaling procedure developed by *Houston et al.* [1998] that removes the effect of earthquake size so that all the time functions can be plotted on the same scale. The time functions can then be grouped in various sets and averaged to investigate how their shapes may vary with depth, region, and earthquake type.

Paper number 2000JB900468.
0148-0227/01/2000JB900468$09.00.

2. Catalog of Source Time Functions

Tanioka and Ruff [1997] (hereinafter referred to as TR) and coworkers in the University of Michigan seismology group determined time functions by inversion of teleseismically recorded body waves recorded by the Global Seismic Network (see TR and *Ruff and Miller* [1994] for details). The body waves (mostly *P* waves) are inverted together for the best fitting point source time function (for a few very large events, a line source was assumed). The procedure involves varying the assumed depth and choosing as the best depth that which minimizes the misfit between observed and synthetic seismograms. TR consider that shallower than 100 km, their depths are better resolved than the automated inversions of the Harvard centroid moment tensor (CMT) catalog, the U. S. Geological Survey moment tensor catalog, and the Earthquake Research Institute CMT catalog, because TR's inversion utilizes higher-frequency data and carefully examines the effect of varying the depth. However, for events deeper than 100 km, TR depths commonly underestimate the Harvard CMT depths, often by 50 to 75 km. This occurs because TR's parameterization of the *P*

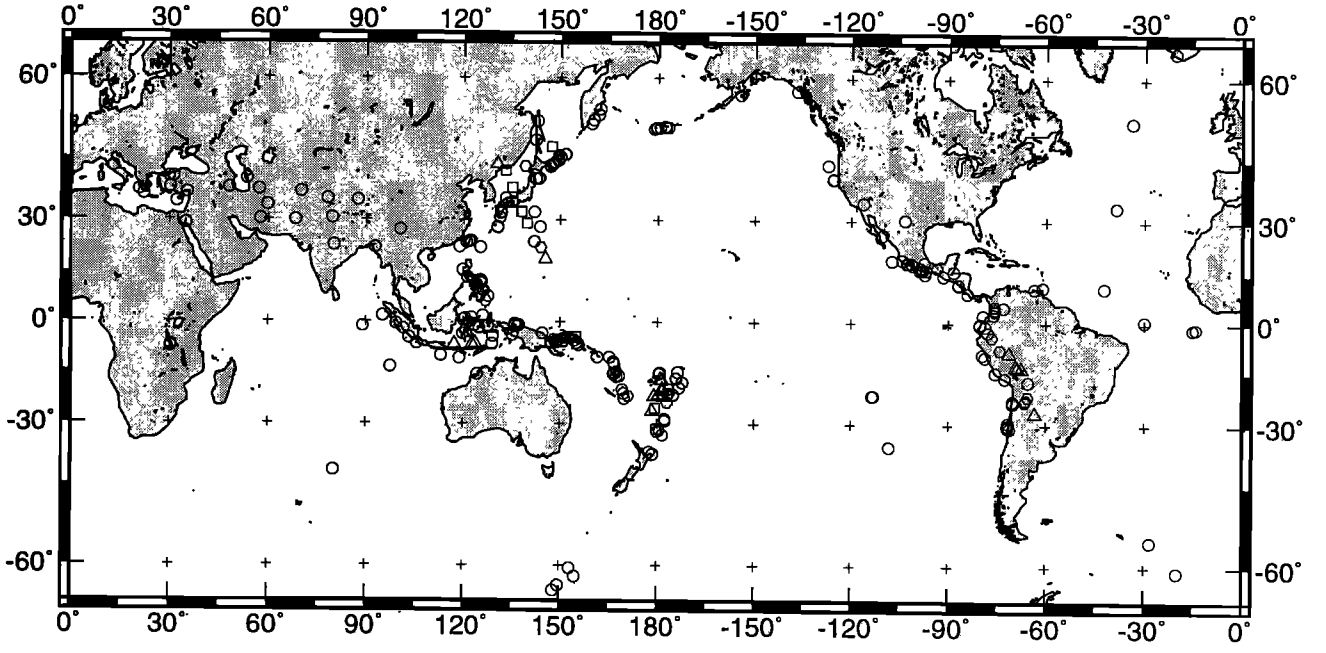

Figure 1. Locations of all earthquakes in this study grouped by depth. Circles represent events with depths <100 km, hexagons events with depths between 100 and 350 km, squares events with depths between 350 and 550 km, and triangles events with depths between 550 and 700 km. For events with TR depths <100 km, the TR depths are used; for deeper events, Harvard CMT depths are used.

wave velocity near the source consists of only three discrete values (6.7, 8.0, or 10.0 km/s) and tends to underestimate the actual velocity near the sources for deep events, resulting in shallower depth estimates. Therefore, for events with TR depths ≥ 100 km, I used Harvard CMT depths.

The files that comprise the catalog of source time functions are available on the Web in ASCII format (at www.geo.lsa.umich.edu/SeismoObs/STF.html) and contain the following information: the focal mechanism assumed for the inversion, number of stations used, inferred duration, inferred depth, body wave moment obtained, and a time series representing the event's time function, determined as described above. The duration, depth, body wave moment, and time function are obtained from the inversion process. The sampling rates of the time series range from 5 samples/s to 0.5 samples/s (only one event at this low sampling rate). To facilitate the computations and comparisons, all time functions in this study were resampled by interpolation to 5 samples/s. The focal mechanism assumed for the body wave inversion comes from one of three sources: the Harvard CMT catalog, the USGS moment tensor catalog, or the Michigan group's own inversions for moment tensor (available on the Web in graphic form at www.geo.lsa.umich.edu/SeismoObs/MTRFs.html).

The catalog contains events from 1991 to the present, although there are only five events from 1991 to 1993, during which time the technique was being developed and Global Seismic Network data were sparse. The completeness of the catalog varies over time, but it appears to be roughly complete for $M_W \geq 6.9$ for 1996 and 1997. About half of the events are smaller than M_W 6.8.

Locations of the 255 events studied here are shown in Figure 1 and given in an electronic supplement along with other event data[1]. Figures 2 and 3 show several time functions from the TR catalog, compared to time functions for the same events inferred from other studies, data, and techniques. Good agreement is seen for the majority of cases.

Some limitations of the catalog should be mentioned. It can be difficult and inherently arbitrary to pick the termination of rupture from these time functions. Time functions obtained with this procedure can have negative values, which are not physically meaningful. Probably the most reliable part is the first peak, which is the part that is used in a study of dynamic stress drop by *Ruff* [1999]. The catalog is an amalgam of results obtained by different researchers, using different sampling rates (in a few cases not as finely as desirable) and different criteria to pick the beginning of the *P*-waves. Nevertheless, the catalog is a unique and valuable resource.

3. Scaling Time Functions to a Common Moment

The seismic moments of the 255 events studied here vary by factors of more than 4000, and consequently, their durations and amplitudes vary greatly. In order to

[1]Supporting data table is available via Web browser or via Anonymous FTP from ftp://kosmos.agu.org, directory "append" (Username = "anonymous", Password = "guest"); subdirectories in the ftp site are arranged by paper number. Information on seraching and submitting electronic supplements is found at http://www.agu.org/pubs/esupp_about.html.

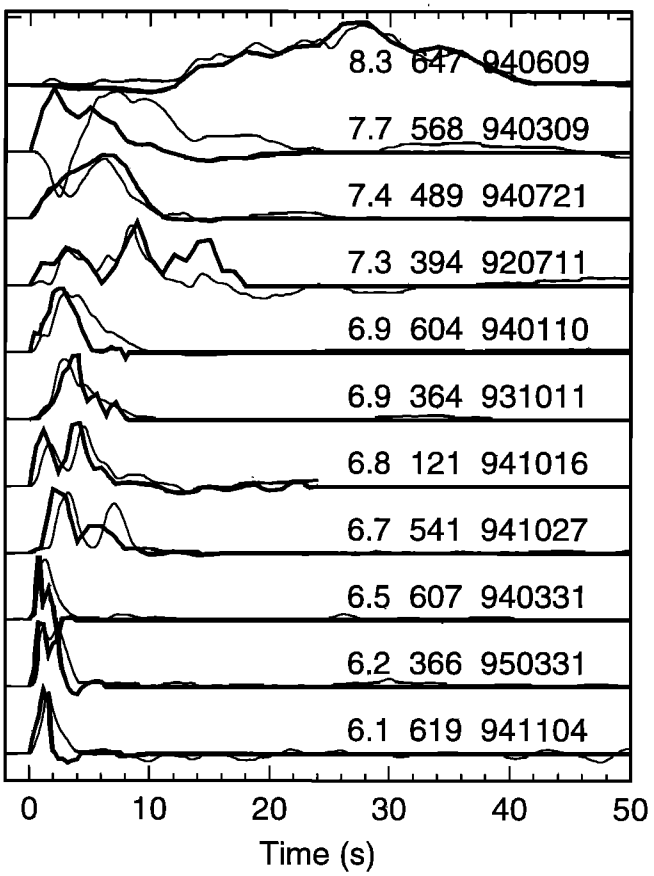

Figure 2. Comparison of source time functions from the TR catalog (thick lines) with broadband stacks from *Houston et al.* [1998] (thin lines) for the 11 events in common. M_W, depth, and date are given for each event. The March 9, 1994, Tonga earthquake had a change in focal mechanism that is evident in the broadband stack.

compare shapes of time functions from earthquakes of widely varying sizes, *Houston et al.* [1998] developed a method for scaling time functions to remove the effect of moment.

3.1 Dependence of Duration on Seismic Moment

The scaling procedure requires assuming how duration depends on seismic moment. If rupture velocity, stress drop, and fault plane aspect ratio are roughly constant with moment, then the definition of moment implies that duration scales as the cube root of moment; this has been found empirically by several studies [e.g., *Kanamori and Anderson*, 1975; *Furumoto and Nakanishi*, 1983; *Vidale and Houston*, 1993; *Abercrombie*, 1995]. However, TR regressed durations, which were estimated subjectively from the time functions, against the body wave moments computed from the time functions, and obtained duration scaling as $M_0^{0.41}$. Figure 4a shows durations versus body wave moments for all events in this study with depths <70 km. The moment dependence is very close to that found by TR. However, Figure 5 illustrates that the TR body wave moments are systematically smaller than the Harvard moments, particularly so for the larger events (those with body wave moments > 8×10^{19} N m). Figure 4b uses the Harvard CMT moments, which are likely more reliable since they are determined from longer-period data; here the dependence of duration on moment is much closer to the theoretically expected exponent of 1/3. When only the events with $M_W \geq 6.2$ are included, which are likely better resolved, the durations scale as $M_0^{0.33}$, the theoretically expected value (Figure 4c). Thus it seems that the most reasonable and conservative approach is to use the theoretically expected, traditional moment scaling. To do this, it is necessary to associate each time function with its Harvard CMT moment and scale the time functions so that the total moment in each equals the CMT moment.

3.2 Moment Scaling and Duration Scaling

To scale the time functions to a common moment, the time axis and the amplitude are simultaneously adjusted, so that the area under the resulting scaled time function is reduced or increased to the same value for all events. This value is the reference value M_{0ref}, here chosen to be 1×10^{19} N m, equivalent to $M_W = 6.6$. The time axis is divided by $(M_0')^{1/3}$, where M_0' is the moment of the ith event. To preserve the relation between moment and area under the time function, amplitudes must be divided by $(M_0')^{2/3}$. This scaling procedure can be generalized in several ways, most simply by dividing the time axis by $(M_0')^x$ and the amplitudes by $(M_0')^{1-x}$, where x is close to, but not necessarily equal to, 1/3. A slightly more complicated procedure is given by TR in a section on "generic source

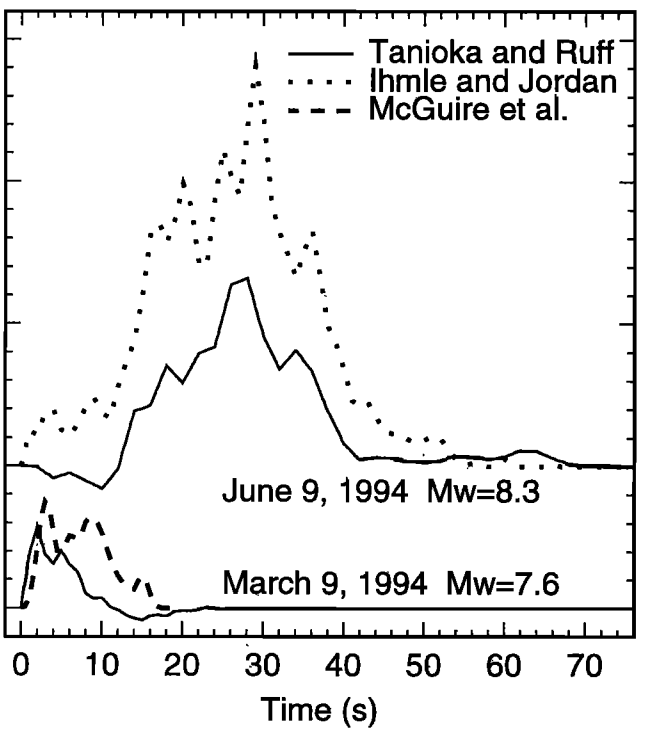

Figure 3. Comparison of source time functions found by *Ihmle and Jordan* [1995] (dotted line) and *McGuire et al.* [1997] (dashed line) with those from the TR catalog (solid lines) for the large deep earthquakes of March 9 and June 9, 1994.

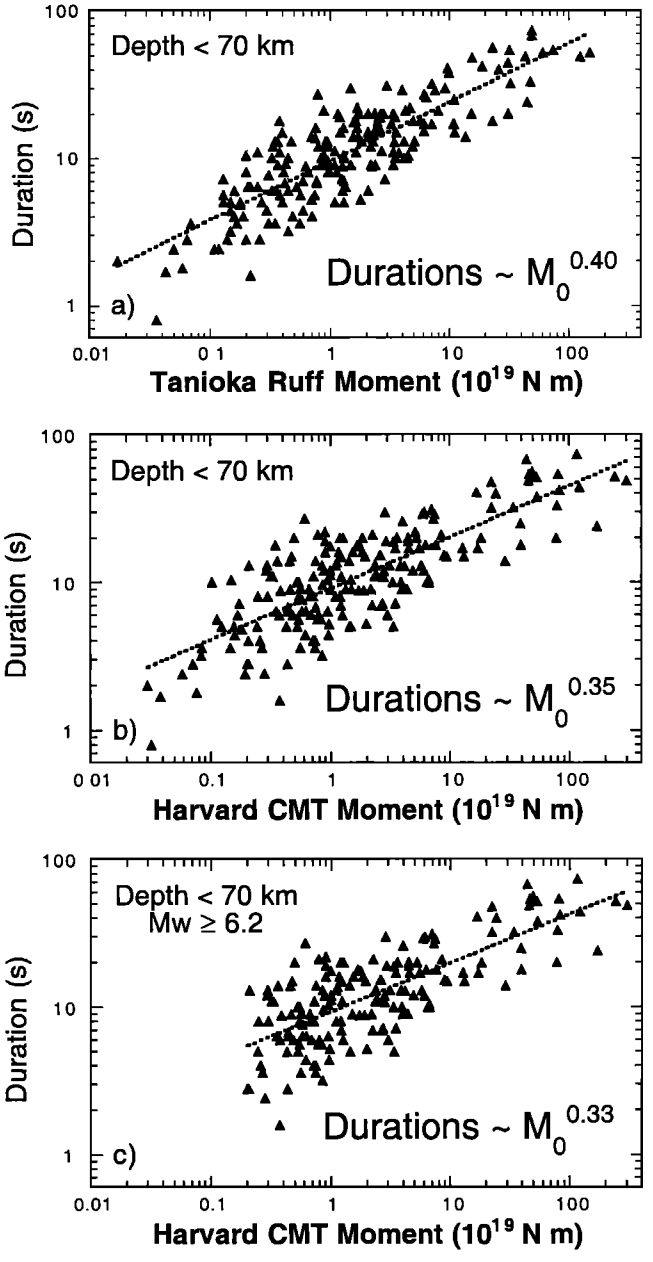

Figure 4. Relation between duration of rupture estimated from body wave inversions by TR and seismic moment for events with TR depth <70 km. The dashed lines show the least squares fits. (a) Durations are proportional to $M_0^{0.40}$ if TR moments are used. (b) Durations are proportional to $M_0^{0.35}$ if Harvard CMT moments are used. (c) Durations are proportional to $M_0^{0.33}$ if Harvard CMT moments are used and events are restricted to those with $M_W \geq 6.2$.

time functions"; it was designed to account for apparent changes in time function shape with moment implied by TR's analysis using TR moments. However, given the results discussed in section 3.1 (i.e., Figures 4 and 5), the standard $M_0^{1/3}$ scaling seems preferrable.

This type of scaling was termed moment scaling by *Houston et al.* [1998], who also described another method for scaling termed duration scaling. In duration scaling, the time axis is adjusted so that the termination of each duration-scaled time function occurs at the same reference duration, and the moment rates are adjusted so that all scaled time functions have the same area underneath. Thus, when duration-scaled time functions are averaged, the long tails that necessarily result from averaging moment-scaled time functions of different durations are avoided. Duration scaling is useful in determining the overall shape of sets of events. A useful way to display the average of duration-scaled time functions is to squeeze or stretch it in time so that its duration equals the average scaled duration of that set of events; the resultant average scaled time function then contains information about both the average shape and scaled duration of that set of events. Further description and examples of moment- and duration-scaling including mathematical formulae are given by *Houston et al.* [1998].

4. Results: Shape and Duration of Scaled Time Functions in TR Catalog

The subsequent analysis reported here was performed with two versions of moment scaling (in addition to duration scaling): (1) scaling time by $M_0^{1/3}$ and amplitude by $M_0^{2/3}$ using Harvard CMT moments (time function amplitudes were scaled to be consistent with the Harvard moments), and (2) scaling time by M00.41 and amplitude by M0(1 - 0.41) using TR moments (in which case time functions were used as is). The results were found to be very similar in all cases, except in the situation with the fewest number of events per group (grouping events by subduction zone). The results discussed below and shown in the figures use the first version of moment scaling. Differences between the two versions of moment scaling are likely to be more important for studies of whether and how event shape changes with moment.

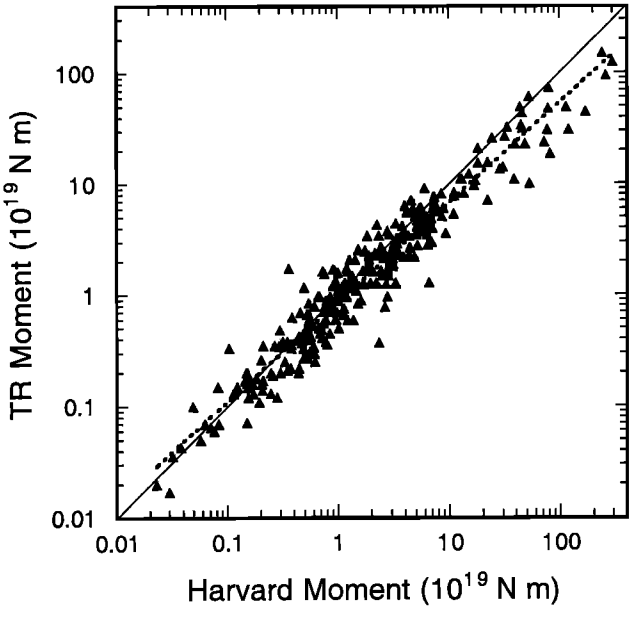

Figure 5. Seismic moment taken from the Harvard CMT catalog versus moment from the TR catalog. For larger events the TR moment systematically underestimates the Harvard moments. The solid line represents equality between the two measures of moment, and the dashed line shows the least squares fit: $M_0^{TR} = 0.860 + (M_0^{Hvd})^{0.8975}$ with $R = 0.928$.

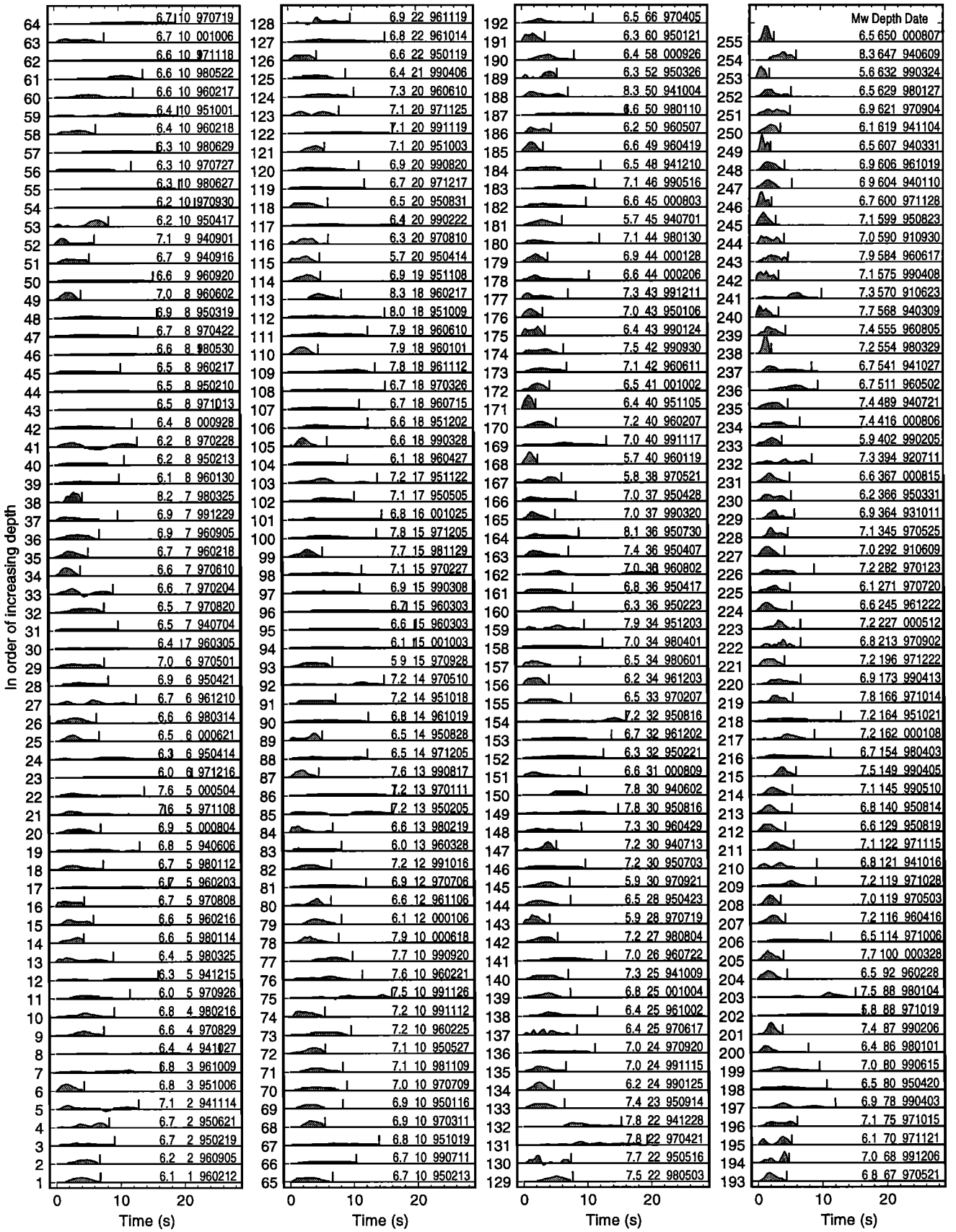

Figure 6. Moment-scaled time functions for all 255 events from the TR catalog in order of increasing depth. For each event M_W, depth, and date are given. For events with TR depths <100 km, the TR depths are used; for other events, Harvard CMT depths are used. Vertical bars show scaled durations, which, although variable, decrease with depth.

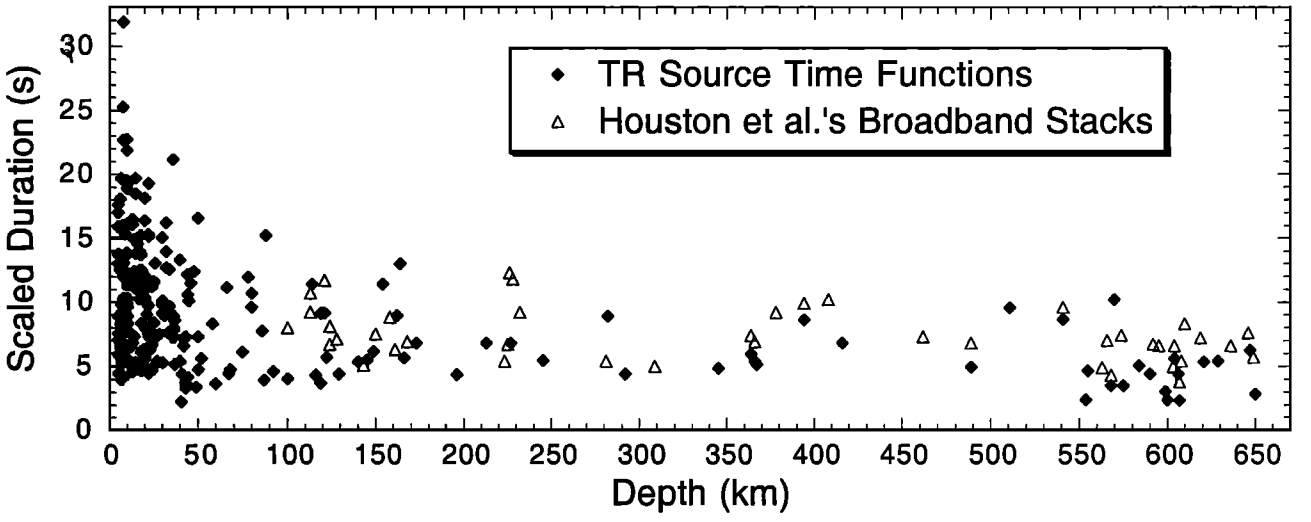

Figure 7. Scaled durations against depth. Durations are scaled by the cube root of moment as described in the text, so that events of different sizes may be compared. A fairly distinct change in duration at 40 km depth is evident for the TR time function catalog. Scaled durations of deep earthquakes based on broadband stacks from *Houston et al.* [1998] are also shown for comparison.

To help ensure higher data quality, in most subsequent calculations in this paper, I excluded events with MW <6.2 (the Harvard CMT moment is used) or TR depth <5 km because in these cases the time functions are probably less reliable. This results in a more reliable subset of 221 time functions of shallow and deep earthquakes that will be used below to investigate variations in time function characteristics with depth and tectonic setting.

4.1 Variations With Depth

All 255 moment-scaled time functions are plotted in order of increasing depth in Figure 6. Each event was moment-scaled to a MW = 6.6 event. A decrease in duration with increasing depth is evident. Event data, including location, depth, seismic moment, number of zero crossings, skewness, focal mechanism type, duration, and scaled duration, are available in the electronic supplement. In Figure 7 scaled durations of the 221 events with MW ≥ 6.2 and TR depth >5 km are plotted against depth (using Harvard CMT depth if TR depth exceeds 100 km), revealing a fairly abrupt decrease in scaled duration around 40 km depth.

Included in Figure 7 for comparison are scaled durations from *Houston et al.* [1998], who analyzed broadband and short-period regional stacks of 42 events that occurred from July 1992 through July 1995. The two independent estimations of durations of deep earthquakes are generally in good agreement. Scaled durations of events at 350 to 550 km depth are longer than expected from either a simple linear trend between the intermediate and deepest events or the trend predicted by a constant stress drop model with rupture velocity proportional to shear wave velocity as it increases through the upper mantle; in Figure 7 an abrupt decrease in duration below 550 km is noticeable. These findings are consistent with key results of *Houston et al.* [1998] and (S. E. Persh and H. Houston, Time functions of deep earthquakes determined from global stacks of GSN broadband records, submitted to *Journal of Geophysical Research*, 2000). However, the number of events in the 350 to 550 km depth range is small because that depth range spans a minimum in seismicity; also there is some overlap between the events studied by *Houston et al.* [1998] and those in the TR catalog.

The change in shape with depth is directly examined in Figure 8 where scaled time functions with $M_W \geq 6.2$ are grouped by depth, and averaged. Above 40 km depth, there appears to be a weak tendency for duration to decrease with depth; this is seen more clearly in section 4.5 which considers only thrust events in subduction zones. The rather abrupt change near 40 km depth is again seen. The average shapes of scaled time functions of deep earthquakes in Figure 8 are generally similar to those found by *Houston et al.* [1998, e.g., see their Figure 13]. I divided the events between 100 and 350 km into two groups, above and below 200 km. The deeper of the two groups has a slightly shorter duration, consistent with a systematic, gradual shortening in duration from 40 to 350 km depth. To summarize Figures 6, 7, and 8, over most depth ranges, scaled durations show a systematic gradual decrease with increasing depth that is expected due to increases in shear wave velocity and hence rupture velocity, but they deviate from such expectations with an abrupt decrease around 40 km, rough constancy between 350 and 550 km, and another abrupt decrease around 550 km.

The abrupt change at 40 km depth may be plausibly related to a change from primarily interplate events at subduction zones, which comprise the largest subset of shallow events, to primarily intraplate events within descending slabs. Indeed, *Tichelaar and Ruff* [1993] found that the downdip edge of the seismogenic interface in most subduction zones lies at a depth of 40 ± 5 km. However, the specific physical cause of the decrease in duration is difficult to establish, as rupture duration is determined by several factors that may trade-off, including

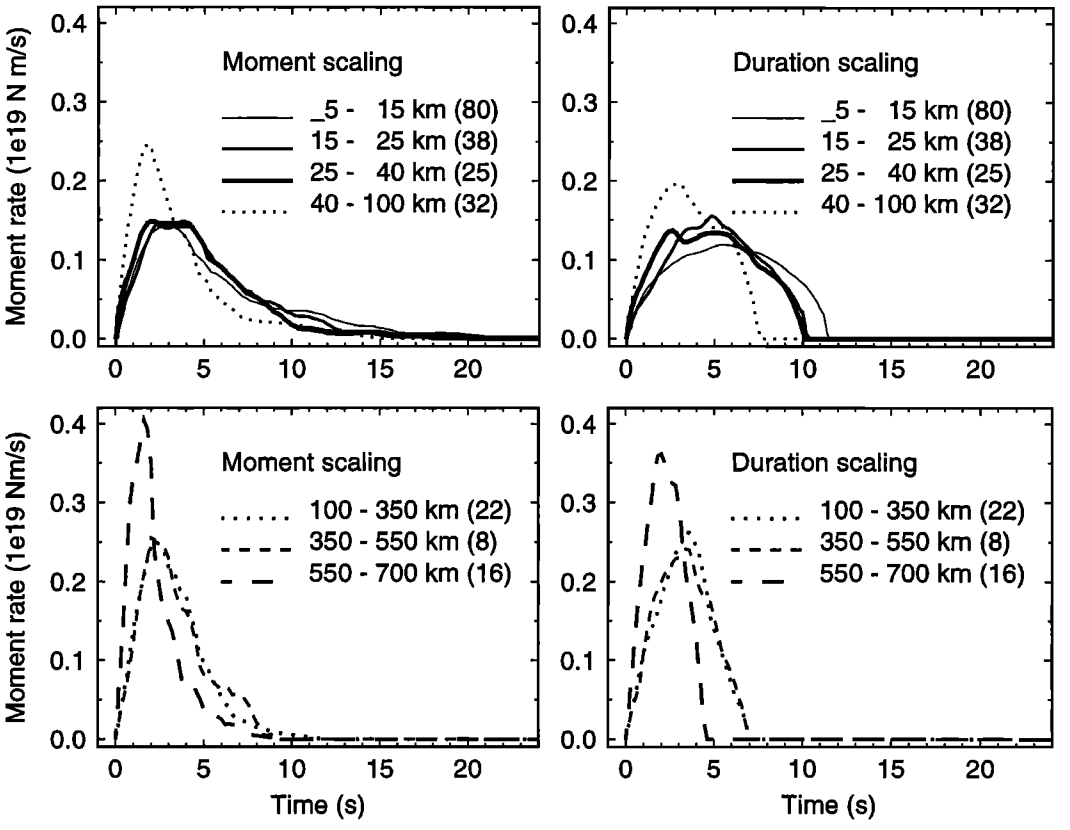

Figure 8. Averages of scaled source time functions grouped according to event depth. (top) Events shallower than 100 km. (bottom) Events deeper than 100 km. (left side) Moment-scaled source time functions. (right side) Duration-scaled source time functions: source time functions were scaled to have the same durations, then averaged; finally, the average was scaled to the average scaled duration for that group. Such a display conveys both the average event shape and scaled duration. Events deeper than 40 km depth are distinctly shorter than shallower ones. Event durations are systematically briefer with increasing depth, except for events in the 350 to 550 km depth range.

stress drop, rigidity and rupture velocity [e.g., *Kanamori and Anderson*, 1975; *Vidale and Houston*, 1993]. A larger stress drop for intraplate events compared to interplate events is commonly invoked [e.g., *Kanamori and Allen*, 1986; *Scholz et al.*, 1986; *Houston*, 1990; *Green and Houston*, 1995]; more recently, lower rigidity for shallow subduction zone events has been proposed as an explanation [*Bilek and Lay*, 1999].

In the depth range 350 to 550 km the deviation from the overall trend of shorter scaled durations with greater depth seen in Figures 7 and 8 is not well understood, and is necessarily delineated by fewer events because that depth range extends over a seismicity minimum. *Houston et al.* [1998] speculated that the longer-than-expected scaled durations could be related to rupture in more heterogeneous material than that above or below, perhaps due to partial transformation in the cold core of subducting slabs of metastable olivine to spinel-structure [e.g., *Frohlich*, 1987, Figure 10]. If so, a different mechanism of faulting below 550 km would be implicated.

4.2 Complexity and Skewness of Time Functions

To examine the shapes of the time functions more closely, I quantified their complexity and calculated their skewnesses. I defined the complexity as the number of subevents (or "bumps") in the time function with roughly similar moment and separated by a substantial fraction of the total duration, as in *Houston et al.* [1998]. The number of bumps can be determined automatically from how many times the time derivative of the moment rate function crosses zero. Each zero crossing represents a change in the slope of the time function from positive to negative, or vice versa. However, the number of zero crossings increases with the overall moment and duration because, although earthquake rupture processes are believed to be generally self-similar, teleseismic seismograms have little energy above 1 Hz due to attenuation in the mantle and crust. Since a measure of complexity independent of overall earthquake moment is desired, the time functions are scaled, then filtered to remove frequencies higher than ~0.5 Hz in scaled frequency (using a cosine taper between 0.3 and 0.6 Hz). Then the time derivative is taken, and the number of zero crossings counted automatically. The number of bumps is given by half of one plus the number of zero crossings.

Figure 9 shows that TR scaled time functions for events smaller than about M_W 6.2 consistently have fewer resolved subevents than the larger events, even though all were filtered as mentioned above. This could indicate that the smaller events tend to be inherently simpler or, more

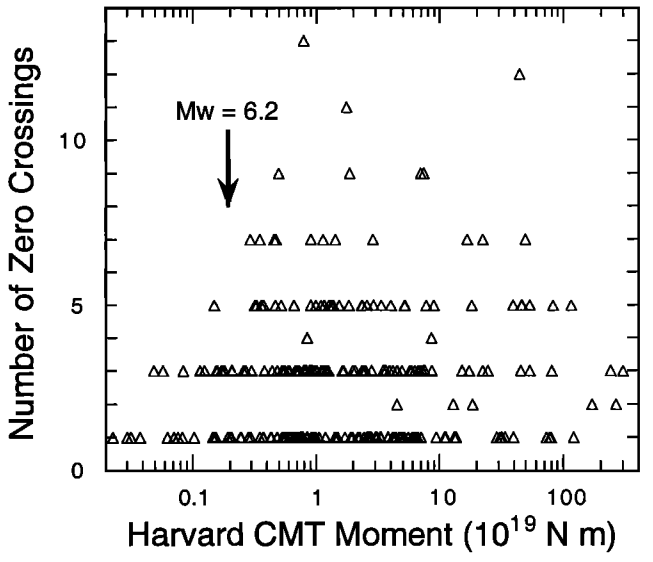

Figure 9. The number of zero crossings of the time derivative of the source time functions, a measure of the complexity or bumpiness of the source time functions, shows little dependence on seismic moment above a threshold moment corresponding to $M_W = 6.2$. Below this threshold, similar complexity may be present in the ruptures but unresolved by the TR inversion of teleseismic waveforms, due to bandwidth limitations.

likely, that their time functions are not as well-resolved relative to their corner frequencies. This is likely to occur because the corner frequencies are too near the high-frequency limit imposed by attenuation of teleseismic waveforms. Thus Figure 9 provides additional support for including only events with $M_W \geq 6.2$ in most parts of this study.

Figure 10 shows how the complexity changes with depth. The mean number of zero crossings for all 221 events with depth >5 km and $M_W \geq 6.2$ is 2.8 (standard error 0.14); for events deeper than 100 km it is 1.9 (standard error 0.17). About 40% of the events have only one zero crossing, i.e., one subevent. In general, the complexity decreases as depth increases, with the most abrupt change seen around 40 km depth. Since interplate events are mainly confined to depths above 40 km [e.g., *Tichelaar and Ruff*, 1993], one interpretation of the change in complexity is that interplate events produce more subevents than intraplate events, perhaps because they occur in the more heterogeneous, rapidly deforming interplate boundary region.

Skewness measures the symmetry of a time series about its centroid time and is computed from the second and third moments about the mean [*Pollard*, 1977]. A skewness of 0 indicates an ideally symmetric time function. Positive skewness indicates that the time function has a tail; negative skewness indicates that more moment release occurs during the latter part of the rupture. The mean skewness of the 221 TR time functions is 0.12; for events deeper than 100 km it is 0.17. That value can be compared to 0.36 for events deeper than 100 km from *Houston et al.* [1998], who obtained time functions of deep events with a stacking technique that likely resolves long low-amplitude tails better. This suggests that the TR time functions may be biased toward lower values of skewness, which is plausible because there is a tendency in the TR catalog to pick the termination of rupture a bit early (e.g., see Figure 15).

4.3 Variations With Focal Mechanism for Shallow Events

The broad effect of tectonic regime on earthquake time histories can be explored by categorizing the 143 shallow events (with 5 km $\leq$ depth $\leq$ 40 km and $M_W \geq 6.2$) according to their focal mechanism type (Figure 11). To categorize the events, I use the P, T, and N axes to define the types of focal mechanisms, rather than strike, dip, and rake. This approach is preferred over definitions using

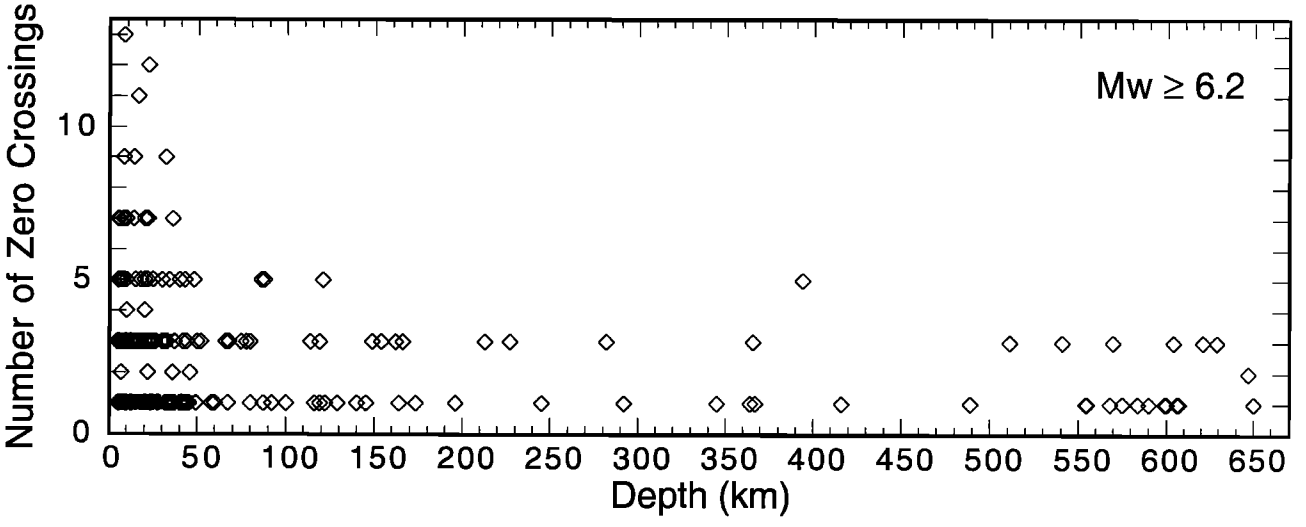

Figure 10. Complexity, as measured by the number of zero crossings of the derivative of the source time functions of events with $M_W \geq 6.2$, decreases as depth increases, with the greatest change occurring around 40 km depth. Scaled time functions were filtered to equalize the effects of attenuation on the shapes of time functions of small and large earthquakes.

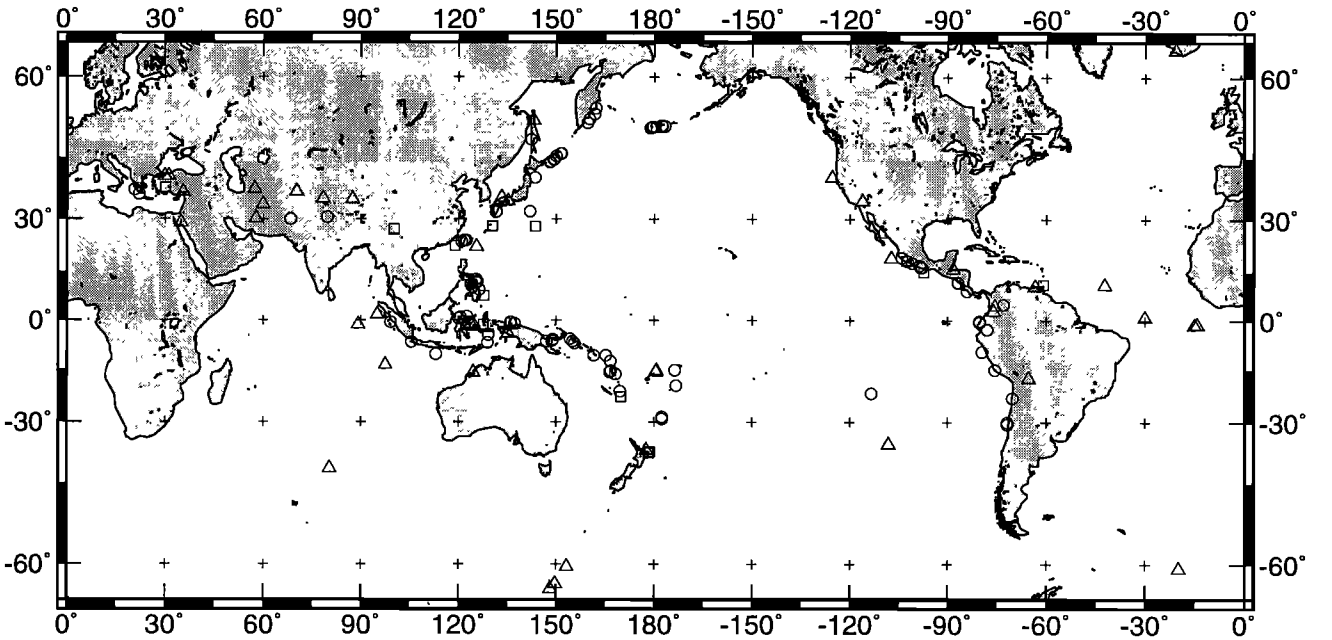

Figure 11. Locations of shallow events (5 km ≤ depth ≤ 40 km) with $M_W \geq 6.2$ according to focal mechanism. Circles, squares, and triangles represent events with thrust, normal, and strike-slip focal mechanisms, respectively.

strike, dip, and rake, which are not orthogonal, because it allows a symmetric treatment of the three types of focal mechanisms [e.g., see *Frohlich and Apperson*, 1992; *Kaverina et al.*, 1996]. Here thrust events are defined as those for which the T axis plunges more steeply than 45°; normal events those for which the P axis plunges >45°; and strike-slip events are those with the N axis plunging >45°. It is possible for focal mechanisms to fall into neither the thrust, normal, nor strike-slip category if all three axes plunge more shallowly than 45° (e.g., they could all have the same plunge of 35.26°); such events are considered oblique. Only one of the 143 shallow events was oblique.

The shapes and durations of the average scaled time functions of thrust and normal earthquakes appear to be somewhat different from that of the strike-slip events (Figure 12). The reasons for this difference are not entirely clear; several competing factors may be at work. Scaling of the length of strike-slip versus dip-slip ruptures has been a topic of continuing discussion, as yet unresolved [e.g., *Scholz*, 1982; *Scholz et al.*, 1986; *Shimazaki*, 1986; *Romanowicz*, 1992; *Scholz*, 1994a; *Romanowicz*, 1994; *Scholz*, 1994b; *Pegler and Das*, 1996]. Strike-slip ruptures are believed to be limited in width by the thickness of the crust and presumably can grow only in length and (disputably) slip as their moment increases; thus, if other factors such as rupture velocity and stress drop are similar for strike-slip and dip-slip ruptures, one would expect strike-slip events with M_W above ~6.6 to have longer durations for a given moment. However, for this data set (Figure 12) the strike-slip events have shorter durations for a given moment; the average scaled duration of the 46 strike-slip events (9.2 s) is 2.4 s shorter than that of the 80 thrust events (11.6 s). The situation is similar for the subset of events with $M_W \geq 7.0$ (containing 14 strike-slip (8.6 s) and 34 thrust events (10.8 s)); even for events with $M_W \geq 7.2$, the average scaled duration of the 10 strike-slip events (9.5 s) remains shorter than that of the 23 correspondingly large thrust events (10.9 s).

It should be noted that scaling of strike-slip ruptures does not appear be entirely well understood; for example, the strike-slip rupture lengths versus moments in Figure 1b of *Pegler and Das* [1996], are better fit by a slope of 1/3 rather than the expected slope of 1/2 or 1, suggesting that fault width may continue to grow somewhat with moment.

My preferred explanation of the durations in Figure 12 is that strike-slip events may tend to have larger stress drops and/or rupture velocities than thrust events; this would lead to shorter durations. Globally, most earthquakes are thrust events and occur in subduction zones. Thus thrust earthquakes tend to be closely related to the most active plate boundaries. Shallow thrust earthquakes occur preferentially on the more active, well-developed large-offset faults associated with subduction zones. This may promote longer duration ruptures. It seems plausible that the large relative plate motions and abundant water in subduction zones could give rise to a weaker rheology, resulting in lower stress drop earthquakes, which would have longer durations for a given moment. Rupture velocities might also be reduced in such a setting. Thus a plausible reason for the longer scaled time functions for thrust-type mechanisms versus strike-slip-type mechanisms is the close association of thrust events with the most active (and submerged) seismic plate boundaries. This explanation would not account for the similar long duration of the normal mechanism events, which constitute, however, the smallest group.

It is also possible that large strike-slip events are more likely than dip-slip events to rupture bilaterally; rupture of a long, narrow strip may be more easily impeded than

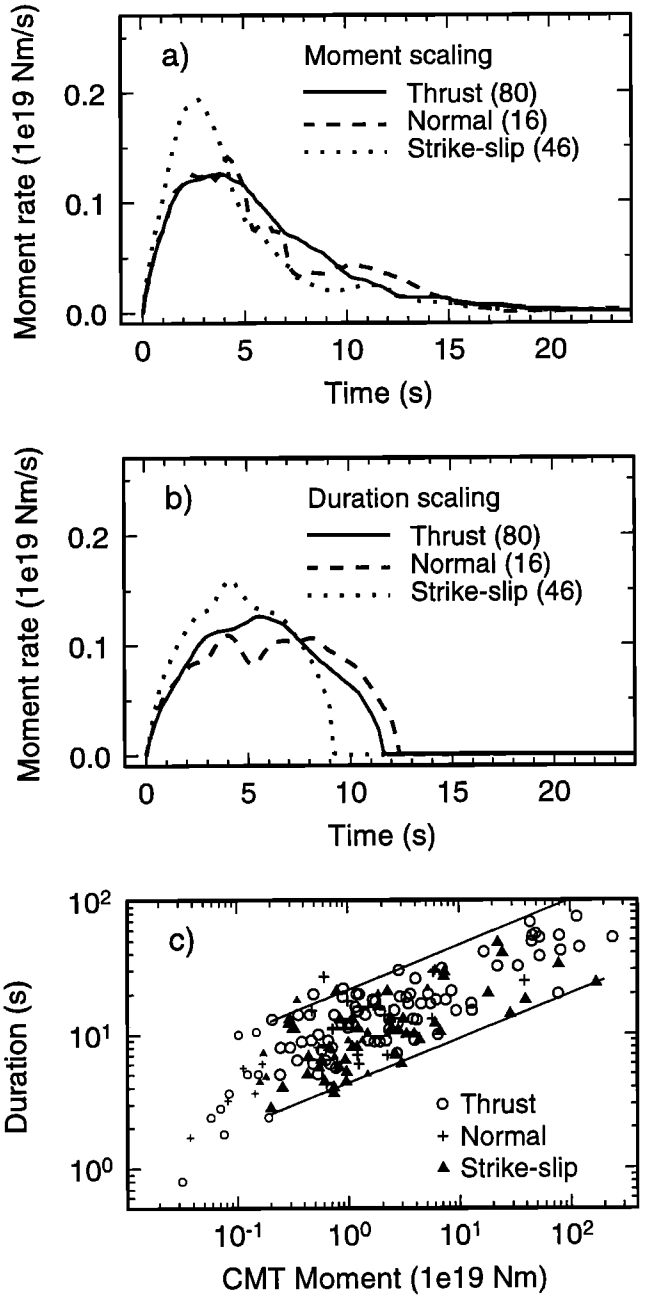

Figure 12. Average scaled time functions of shallow events (depth ≤ 40 km) according to focal mechanism. (a) Moment-scaled time functions of events with $M_W \geq 6.2$. (b) Duration-scaled time functions with $M_W \geq 6.2$. (c) Open circles, crosses, and solid triangles represent events with thrust, normal, and strike-slip focal mechanisms, respectively. Smaller symbols represent events with M_W <6.2 or depth <5 km (i.e., events not included in Figures 12a and 12b). The lines have a slope of 1/3.

rupture of an equant area, so a bilateral nature may be more important in promoting continued rupture growth for strike-slip compared to dip-slip events. A further possibility is that strike-slip events tend to be complex with several subevents, and the termination picked in the TR catalog for complex events may often be earlier than the actual termination due to the difficulty resolving late pulses of moment release. This again points up the difficulty of defining the termination of rupture.

4.4 Variations Between Interplate and Intraplate Thrust Events and Between Subduction Zones

The 80 shallow thrust events (with 5 km ≤ depth ≤ 40 km and $M_W \geq 6.2$) were further divided into 69 events associated with an active subduction zone, in which case they were considered plate boundary events, and 11 others, considered non-plate-boundary events (Figures 13a and 13b). The plate boundary events were required to lie within 100 km of an active subduction zone (with the downgoing plate oceanic) and to possess a CMT focal mechanism consistent with underthrusting on that zone; they are not necessarily exactly on the plate interface, which is difficult to determine precisely in these types of studies. The plate boundary events typically have longer scaled durations than the non-plate-boundary events (Figures 13a - 13d).

A plausible reason for the difference involves the notion discussed above that interplate events have lower stress drops and longer durations than intraplate events. Several studies have presented evidence in support of a distinction between interplate and intraplate faulting [e.g., *Kanamori and Allen*, 1986; *Scholz et al.*, 1986; *Houston*, 1990; *Green and Houston*, 1995]. Further, the interplate subuction zone events studied here occur on or near plate boundaries that are deforming rapidly and in the presence of large amounts of water.

The plate boundary events were further divided into specific subduction zones, including Central America, the Aleutians, the Kuriles (including Kamchatka), Vanuatu, and Tonga-Kermadec. Although the numbers of events in each subduction zone are small, there appears to be a difference in the shape and duration of the average scaled time functions in various zones (Figures 13e and 13f). It is interesting to compare the Central American and Tongan zones. Although the average Central American duration is much longer, the average Central American time function has lower skewness than that of the Tongan time function. If the second version of moment scaling is applied (scaling time by $M_0^{0.41}$ and amplitude by $M_0^{0.59}$ using the TR moments), then the average Central American time function is no longer so distinct from the others, but the Tonga time function is little changed and remains the shortest. The relative skewnesses remain about the same. Time functions from the Vanuatu zone contrast with those from Central America in a different way and appear to be the most complex. Although not shown, time functions from South America were also examined as a group and are similar to those from the Aleutians.

These differences in time functions are suggestive of regional differences in some aspect of the rheology of the plate interface, such as differences in the asperity size or strength distribution [*Ruff*, 1992]. It should also be noted that the depths of the Central American events (8, 10, 10, 15, 15, 18, 18, 20, 23, 27, 31 km) are mostly smaller than those of the Tonga events (24, 30, 33, 36 km) (Figure 13a), consistent with the finding by *Tichelaar and Ruff* [1993] that the down-dip edge of the seismogenic plate interface in Mexico is anomalously shallow, at ~25 km depth. The difference in event depths could explain much of the

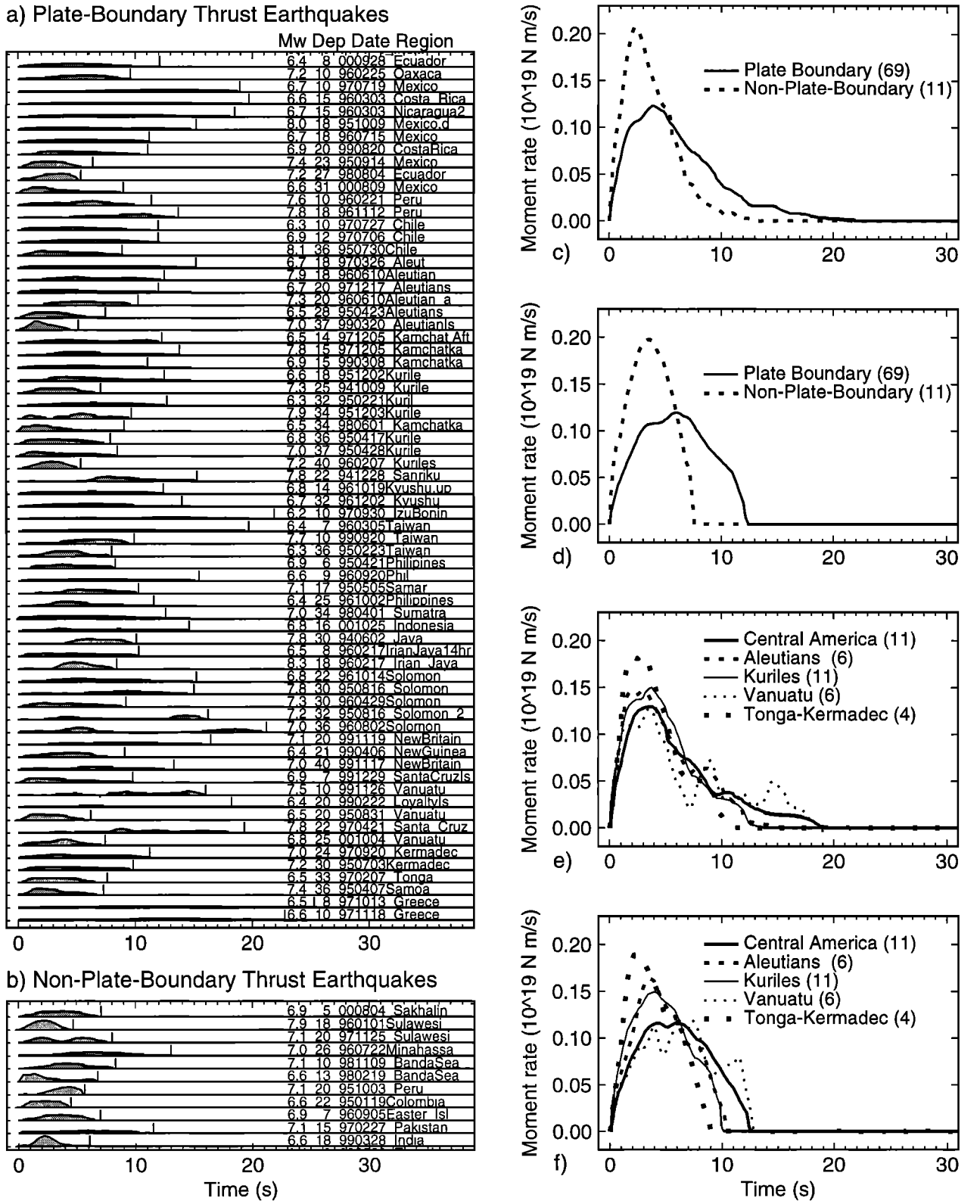

Figure 13. Scaled source time functions of shallow thrust events with $M_W \geq 6.2$. (a) Moment-scaled time functions of events on or near (within 100 km) an interplate boundary. Vertical bars show scaled durations. (b) Moment-scaled time functions of events not on or near a plate boundary. (c) Average moment-scaled time functions for plate boundary and non-plate-boundary events. (d) Average duration-scaled time functions for plate boundary and non-plate-boundary events. (e) Average moment-scaled time functions for several subduction zones. (f) Average duration-scaled time functions for several subduction zones.

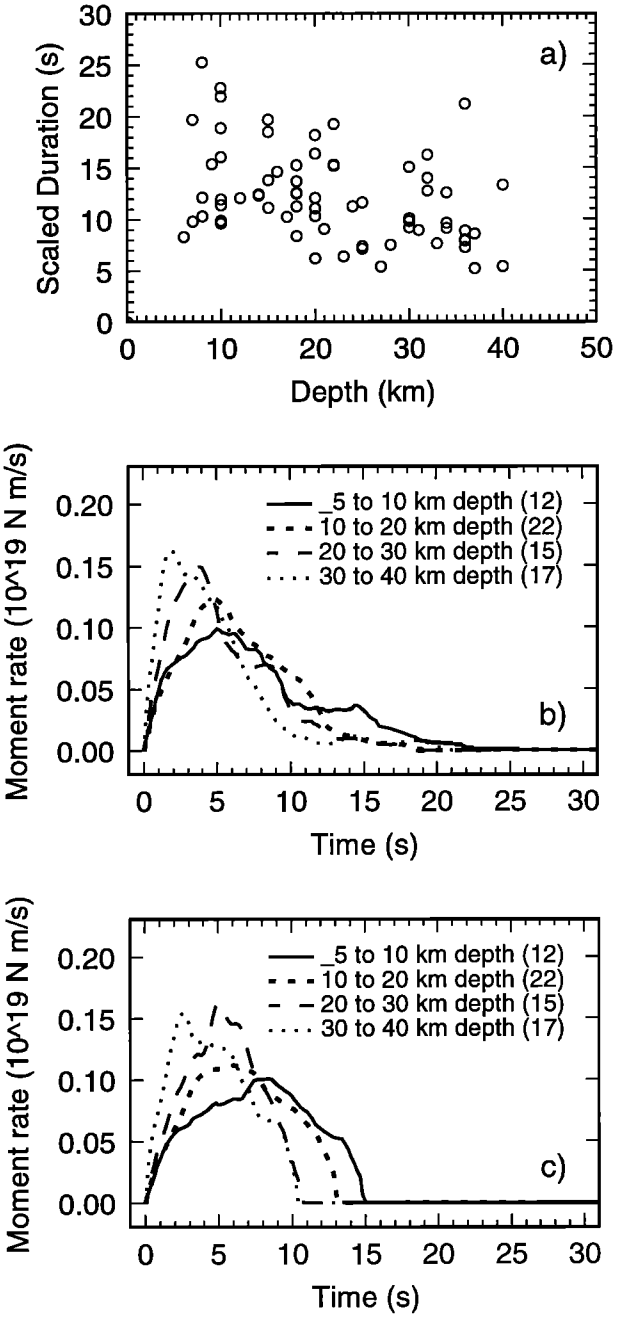

Figure 14. Thrust plate-boundary events with $M_W \geq 6.2$. Scaled durations decrease with depth by a factor of about 1.5, in contrast to a larger change seen by *Bilek and Lay* [1999]. (a) Scaled durations versus depth. (b) Average moment-scaled time functions grouped by depth. (c) Average duration-scaled time functions grouped by depth.

difference between the average time functions for the two zones (compare to Figure 14c), although this is in itself indicative of a major difference between the zones.

Regional differences between the number of aftershocks of large earthquakes in subduction zones have been found by *Singh and Suarez* [1988]. After correcting for the mainshock size, they found variations of more than a factor of 10 in numbers of aftershocks with $m_b \geq 5.0$; in particular, there were many more aftershocks of Tonga-Kermadec mainshocks than of Central American mainshocks, as well as more aftershocks than average in the western Pacific and fewer than average in the eastern Pacific subduction zones. They interpreted this in terms of weaker plate coupling and greater heterogeneity in the western Pacific zones. *Bilek and Lay* [1999] obtained time functions of shallow subduction zone events and found different patterns of decrease in scaled duration with depth for different zones, suggesting variations in rheology between zones.

4.5 Variations With Depth for Shallow Thrust Events in Subduction Zones

Although variations with depth in time function shape and duration for the whole catalog are discussed in section 4.1, it is interesting to examine variations in time function shape and duration above 40 km depth for thrust events on subduction zones. In Figure 13a the scaled time functions of the 69 thrust "plate boundary" events are ordered by increasing depth within each subduction zone. In many cases, for example, for the Central American, Aleutian, and Tonga events, scaled durations decrease systematically with depth within a zone (several similar cases were noted by *Ruff* [1999]). Figure 14 shows that subduction zone thrust events above 20 km have substantially longer durations than those below. In Figure 8 this trend was obscured by shallow strike-slip and intraplate thrust events which are distinctly shorter in scaled duration (Figures 12, 13c, and 13d).

For the subduction zone events alone (Figure 14), there is a significant change between events at depths of 5 to 10 km and deeper ones. However, these results differ somewhat from those of *Bilek and Lay* [1999], who found a much larger decrease (a factor of 2 to 3) in scaled duration with depth over this range, concentrated near 10 to 15 km depth. The discrepancy could be related to the fact that most of their events are smaller than the ones studied here. Indeed, all their events with anomalously long scaled durations (as well as most of their events with anomalously short scaled durations) have moments smaller than 4×10^{18} N m, near the lower size limit of this study. Thus the dramatic decrease in scaled duration near 10 to 15 km depth that they find seems to occur mainly for events smaller than about M_W 6.3. It is more difficult to resolve the time functions of smaller earthquakes, which are more often contaminated by noise; Bilek and Lay's sampling rate is once per second so some of their smaller events are said to terminate after only two or three samples. Figure 15 compares the TR time functions with the durations determined by *Bilek and Lay* [1998, 1999] for all events in common. In general, the TR durations (vertical bars in Figure 15) last significantly longer; furthermore, for the two largest earthquakes, it appears that Bilek and Lay entirely missed the main moment release. Even the TR durations appear to have been picked somewhat early in the time functions (Figure 15), illustrating again the inherent ambiguity in picking the termination of rupture from a typical time function.

5. Conclusions

A systematic analysis of TR's time function catalog reveals an abrupt decrease in the scaled duration of time

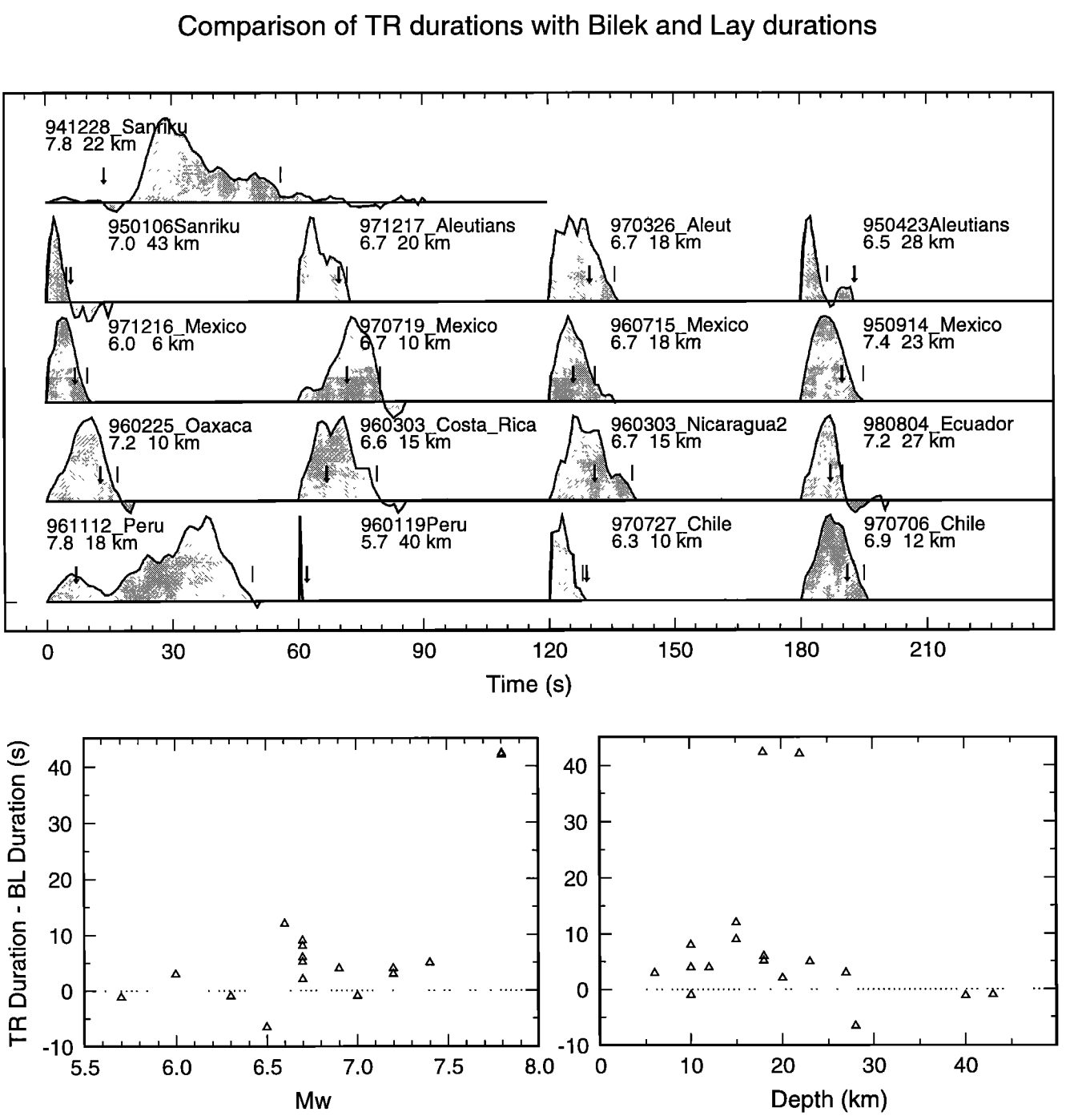

Figure 15. Comparison of TR durations with durations from *Bilek and Lay* [1998, 1999]. (top) TR source time functions for the 17 events in common between this study and *Bilek and Lay* [1998, 1999]. Vertical lines show TR durations; vertical arrows show Bilek and Lay's durations. Event date and name, M_W, and depth (from TR) are given. (bottom) The difference between TR durations and Bilek and Lay's durations versus M_W and depth. Note that Bilek and Lay's durations are generally significantly shorter than TR durations; two events have a difference of more than 40 s and six more events have a difference $\geq$ 5 s.

functions at about 40 km, against a background of more gradual decreases above and below that depth, which is believed to be the maximum depth of interplate seismic coupling. Additionally, events in the depth range 350 to 550 km, consistent with *Houston et al.* [1998], do not conform to expectations of steadily shortening durations with increasing depth. The relationship between interplate and intraplate thrust events is similar to that between all events above and below 40 km depth, as well as to that between thrust and strike-slip earthquakes. These changes in the average scaled time functions of shallow earthquakes may be explained if earthquakes in tectonically active settings tend to be longer in duration and possess longer tails than intraplate events or those in

less active tectonic regimes. Regional variations between subduction zones in time function shape and duration imply that physical differences between interplate surfaces in subduction zones lead to differences in rupture processes. The average time function shapes may be useful for a variety of studies, including those modeling dynamic rupture.

Acknowledgments. I thank L. Ruff, Y. Tanioka, and graduate students at the University of Michigan for making their catalog of time functions so readily available. Helpful reviews of the manuscript were provided by AE S. Schwartz, L. Ruff, an anonymous referee, and S. Persh. The Harvard CMT catalog was used extensively. This work was supported in part by NSF grant EAR-9601979 to H.H.

References

Abercrombie, R.E., Earthquake source scaling relationships from -1 to 5 M_L using seismograms recorded at 2.5 km depth, *J. Geophys. Res.*, *100*, 24,015-24,036, 1995.

Bilek, S.L., and T. Lay, Variation of interplate fault zone properties with depth in the Japan subduction zone, *Science*, *281*, 1175-1178, 1998.

Bilek, S.L., and T. Lay, Rigidity variations with depth along interplate megathrust faults in subduction zones, *Nature*, *400*, 443-446, 1999.

Frohlich, C., Aftershocks and temporal clustering of deep earthquakes, *J. Geophys. Res.*, *92*, 13,944-13,957, 1987.

Frohlich, C., and K.D. Apperson, Earthquake focal mechanisms, moment tensors and the consistency of seismic activity near plate boundaries, *Tectonics*, *11*, 279-296, 1992.

Furumoto, M., and I. Nakanishi, Source times and scaling relations of large earthquakes, *J. Geophys. Res.*, *88*, 2191-2198, 1983.

Green, H.W., and H. Houston, The mechanics of deep earthquakes, *Annu. Rev. Earth Planet. Sci.*, *23*, 169-213, 1995.

Houston, H., A comparison of broadband source spectra, seismic energies, and stress drops of the 1989 Loma Prieta and 1988 Armenian earthquakes, *Geophys. Res. Lett.*, *17*, 1413-1416, 1990.

Houston, H., H.M. Benz, and J.E. Vidale, Time functions of deep earthquakes from broadband and short-period stacks, *J. Geophys. Res.*, *103*, 29,895-29,913, 1998.

Ihmle, P.F., and T.H. Jordan, Source time function of the great 1994 Bolivia deep earthquake by waveform and spectral inversions, *Geophys. Res. Lett.*, *22*, 2253-2256, 1995.

Kanamori, H., Rupture process of subduction zone earthquakes, *Annual Reviews of Earth and Planetary Sciences*, *14*, 293-322, 1986.

Kanamori, H., and C. Allen, Earthquake repeat time and average stress drop, in *Earthquake Source Mechanics, Geophys. Monogr. Ser.*, vol. 37,edited by S. Das, J. Boatwright, and C. Scholz, pp. 227-235, AGU, Washington, D. C., 1986.

Kanamori, H., and D.L. Anderson, Theoretical basis for some empirical relations in seismology, *Bull. Seismol. Soc. Am.*, *65*, 1073-1095, 1975.

Kaverina, A.N., A.V. Lander, and A.G. Prozorov, Global creepex distribution and its relation to earthquake source geometry and tectonic origin, *Geophys. J. Int.*, *125*, 249-265, 1996.

McGuire, J.J., D.A. Wiens, P.J. Shore, and M.G. Bevis, The March 9, 1994 (M_W 7.6) deep Tonga earthquake: Rupture outside the seismically active slab, *J. Geophys. Res.*, *102*, 15,163-15,182, 1997.

Pegler, G., and S. Das, Analysis of the relationship between seismic moment and fault length for large crustal strike-slip earthquakes between 1977-1992, *Geophys. Res. Lett.*, *23*, 905-908, 1996.

Pollard, J.H., *A Handbook of Numerical and Statistical Techniques*, Cambridge Univ. Press, New York, 1977.

Romanowicz, B., Strike-slip earthquakes on quasi-vertical transcurrent faults: Inferences for general scaling relations, *Geophys. Res. Lett.*, *19*, 481-484, 1992.

Romanowicz, B., A reappraisal of large earthquake scaling - Comment, *Bull. Seismol. Soc. Am.*, *84*, 1675-1676, 1994.

Ruff, L.J., Asperity distributions and large earthquake occurrence in subduction zones, *Tectonophysics*, *211*, 61-83, 1992.

Ruff, L.J., Dynamic stress drop of recent earthquakes: Variations within subduction zones, *Pure Appl. Geophys.*, *154*, 409-431, 1999.

Ruff, L.J., and A.D. Miller, Rupture process of large earthquakes in the northern Mexico subduction zone, *Pure Appl. Geophys.*, *142*, 101-172, 1994.

Scholz, C.H., Scaling laws for large earthquakes: Consequences for physical models, *Bull. Seismol. Soc. Am.*, *72*, 1-14, 1982.

Scholz, C.H., A reappraisal of large earthquake scaling, *Bull. Seism. Soc. Am.*, *84*, 215-218, 1994a.

Scholz, C.H., A reappraisal of large earthquake scaling - Reply, *Bull. Seismol. Soc. Am.*, *84*, 1677-1678, 1994b.

Scholz, C.H., C.A. Aviles, and S.G. Wesnousky, Scaling differences between large interplate and intraplate earthquakes, *Bull. Seismol. Soc. Am.*, *76*, 65-70, 1986.

Shimazaki, K., Small and large earthquakes: The effects of the thickness of the seismogenic layer and the free surface, in *Earthquake Source Mechanics, Geophys. Monogr. Ser.*, vol. 37, edited by S. Das, J. Boatwright, and C. Scholz, pp. 209-216, AGU, Washington D. C., 1986.

Singh, S.K., and G. Suarez, Regional variation in the number of aftershocks ($m_b \geq 5$) of large, subduction-zone earthquakes ($M_W \geq 7.0$), *Bull. Seismol. Soc. Am.*, *78*, 230-242, 1988.

Tanioka, Y., and L. Ruff, Source time functions, *Seismol. Res. Lett.*, *68*, 386-400, 1997.

Tichelaar, B.W., and L.J. Ruff, Depth of seismic coupling along subduction zones, *J. Geophys. Res.*, *98*, 2017-2037, 1993.

Vidale, J.E., and H. Houston, The depth dependence of earthquake duration and implications for rupture mechanisms, *Nature*, *365*, 45-47, 1993.

H. Houston, Department of Earth and Space Sciences, University of California, Los Angeles, 595 Young Dr. East, Los Angeles, CA 90095-1567. (hhouston@ess.ucla.edu)

(Received April 19, 2000; revised December 12, 2000;
accepted December 14, 2000.)